

# Kiloparsec-Scale Jets in FR I Radio Galaxies and the $\gamma$ -ray Background

L. Stawarz<sup>1</sup>

*Max-Planck-Institut für Kernphysik, PO Box 103980, 69029 Heidelberg, Germany*

Lukasz.Stawarz@mpi-hd.mpg.de

T. M. Kneiske

*Department of Physics and Mathematical Physics, University of Adelaide, North Terrace,  
Adelaide, SA 5005, Australia*

tkneiske@physics.adelaide.edu.au

J. Kataoka

*Department of Physics, Tokyo Institute of Technology, 2-12-1, Ohokayama, Meguro, Tokyo  
152-8551, Japan*

kataoka@hp.phys.titech.ac.jp

## ABSTRACT

We discuss the contribution of kiloparsec-scale jets in FR I radio galaxies to the diffuse  $\gamma$ -ray background radiation. The analyzed  $\gamma$ -ray emission comes from inverse-Compton scattering of starlight photon fields by the ultrarelativistic electrons whose synchrotron radiation is detected from such sources at radio, optical and X-ray energies. We find that these objects, under the minimum-power hypothesis (corresponding to a magnetic field of  $300 \mu\text{G}$  in the brightest knots of these jets), can contribute about one percent to the extragalactic  $\gamma$ -ray background measured by EGRET. We point out that this result already indicates that the magnetic fields in kpc-scale jets of low-power radio galaxies are not likely to be smaller than  $10 \mu\text{G}$  on average, as otherwise the extragalactic  $\gamma$ -ray background would be overproduced.

*Subject headings:* radiation mechanisms: non-thermal — galaxies: active — galaxies: jets — gamma-rays: theory

---

<sup>1</sup>also at Obserwatorium Astronomiczne, Uniwersytet Jagielloński, ul. Orła 171, 30-244 Kraków, Poland; stawarz@oa.uj.edu.pl

## 1. Introduction

Observations by the EGRET instrument on board the CGRO have established presence of isotropic extragalactic background radiation in the 100 MeV – 10 GeV photon energy range, with an integrated flux  $I(> 100 \text{ MeV}) \lesssim 10^{-5} \text{ ph cm}^{-2} \text{ s}^{-1} \text{ sr}^{-1}$  and a curved (concave) spectrum (Sreekumar et al. 1998; Strong et al. 2004). It has been argued (Dermer & Schlickeiser 1992; Stecker et al. 1993; Padovani et al. 1993; Salamon & Stecker 1994; Setti & Woltjer 1994; Chiang et al. 1995; Erlykin & Wolfendale 1995; Stecker & Salamon 1996; Chiang & Mukherjee 1998; Weferling & Schlickeiser 1999; Mucke & Pohl 2000), that the bulk of this emission most likely originates from unresolved blazars, whose properties are similar to those detected by EGRET (von Montigny et al. 1995; Hartman et al. 1999). However, as the internal parameters and cosmological distribution of EGRET-like blazar sources are not precisely known, the origin of the diffuse  $\gamma$ -ray background is still being debated, and new classes of objects emitting GeV photons can be analyzed in this context (e.g., Loeb & Waxman 2000; Gabici & Blasi 2003).

Here we discuss the issue of high-energy  $\gamma$ -ray emission from the kiloparsec-scale jets in FR I radio galaxies, and in particular its contribution to the  $\gamma$ -ray background radiation as measured by EGRET. Our study is stimulated by recent results from the Chandra X-ray Observatory, which have shown that X-ray jet emission is common in FR I sources (Hardcastle et al. 2001, 2002, 2003, 2005; Harris et al. 2002a,b; Kataoka et al. 2003; Kraft et al. 2002; Marshall et al. 2002; Wilson & Yang 2002; Worrall et al. 2001, 2003). The established synchrotron origin of this X-ray emission (see all the references above<sup>1</sup>) implies that the kpc-scale jets in FR I radio galaxies will, at some level, be sources of high- and very high-energy  $\gamma$ -ray emission due to the inverse-Compton scattering of ambient (galactic) photon fields by the synchrotron-emitting electrons. This problem was discussed by Stawarz et al. (2003), and considered in more detail for the specific case of the radio galaxy M 87 by Stawarz et al. (2005). The aim of our study — which is an extension of the previous analysis — is twofold, namely an estimation of the aforementioned contribution (taking into account effects of absorption and subsequent re-processing of  $\gamma$ -ray photons by infrared-to-ultraviolet background radiation), and discussion of the constraints on the jet parameters which can be imposed in this way.

The paper is organized as follows. In the next section we describe the ingredients of the model developed to estimate the contribution of kpc-scale FR I jets to the  $\gamma$ -ray background.

---

<sup>1</sup>We note that the origin of the X-ray emission in powerful large-scale jets in quasars is still under debate (see the discussion in Kataoka & Stawarz 2005, and references therein), but the synchrotron scenario for the X-ray FR I jets is widely accepted.

In section 3 we present the results, and discuss briefly the possibility of the direct observation of  $\gamma$ -rays from these sources. General discussion and the main conclusions are presented in section 4. Throughout the paper we assume a cosmology with  $\Omega_M = 0.27$ ,  $\Omega_\Lambda = 0.73$ , and  $H_0 = 71 \text{ km s}^{-1} \text{ Mpc}^{-1}$ .

## 2. The Model

Below we describe the procedure used to estimate the  $\gamma$ -ray emission from a ‘typical’ kpc-scale jet in a FR I radio galaxy. We assume that all of these objects have similar properties, and that the detection rate of their brightest knots at optical and X-ray frequencies depends solely on the amount of relativistic beaming (Sparks et al. 1995; Scarpa & Urry 2002; Jester 2003). Within this approach, we find the ‘universal’ electron energy distribution in the brightest knots of these jets by fitting a broken power-law to the radio-to-X-ray synchrotron continua of the collected jet sources. Next, we compute the  $\gamma$ -ray emission due to inverse-Compton (IC) scattering of the re-constructed universal electron energy distribution on the starlight radiation of the host galaxies (Stawarz et al. 2003, 2005). We include both the Klein-Nishina effects and the relativistic bulk velocity of the emitting plasma in the analysis. We also present the adopted approach in relating the  $\gamma$ -ray output of the jets with the total radio luminosities of the analyzed sources, and hence the  $\gamma$ -ray luminosity function (GLF) of kpc-scale FR I jets with the radio luminosity function (RLF) of low-power radio galaxies (Willott et al. 2001). Finally, we briefly describe the adopted model for the absorption of the emitted high-energy  $\gamma$ -ray photons by the infrared-to-ultraviolet metagalactic radiation field (MRF), taking into account evolution of the background photon field up to high redshifts (Kneiske et al. 2002, 2004), and also re-processing of the absorbed  $\gamma$ -ray photons to lower energies by the cascading processes.

### 2.1. Jet $\gamma$ -ray Emission

We collate data for all FR I radio galaxies with detected X-ray jets. We restrict our analysis to the brightest knots in these jets, which are placed at  $\sim 1$  kpc from the galactic nuclei, thus obtaining a list of 11 sources. Table 1 summarizes the input parameters for the considered knots, i.e., the radio fluxes  $S_R$  as measured at  $\nu_R = 5 \text{ GHz}$ , the optical fluxes  $S_O$  (if available) at  $\nu_O = 5 \times 10^{14} \text{ Hz}$ , and the X-ray fluxes  $S_X$  at  $h\nu_X = 1 \text{ keV}$  photon energies. We fit broken power-laws to the radio-to-X-ray continua of the analyzed knots, with spectral indices  $\alpha_R$  and  $\alpha_X$  measured directly from the data or, when large uncertainties are encountered, with the adopted median values  $\alpha_R = 0.75$  and  $\alpha_X = 1.2$ . We assume a spherical

geometry of radius 26 pc for all knots, which corresponds to an angular radius of  $0.3''$  at the distance of M 87 (see in this context Kataoka & Stawarz 2005). The obtained values of the break frequencies in the synchrotron spectra,  $\nu_{\text{br}}$ , as well as the equipartition magnetic field computed for no relativistic beaming,  $B_{\text{eq}}(1)$ , are also given in Table 1, together with the radio luminosity of the whole source,  $L_{\text{tot}}$ , as given by Liu & Zhang (2002) after conversion to our adopted cosmology and an observation frequency of 5 GHz (assuming a radio spectral index for the whole source of 0.8; see Willott et al. 2001). Finally, in Table 1 we give the estimated value of the ratio between the 5 GHz luminosity of each analyzed knot and the 5 GHz total luminosity of the source,

$$\eta \equiv \frac{4\pi d_L^2 \times [\nu_{\text{R}} S_{\text{R}}]}{L_{\text{tot}}} \quad . \quad (1)$$

The fitting procedure described above allows us to find the ‘typical’ parameters of the brightest knots in FR I radio galaxies, which we adopt hereafter. Besides the spectral indices,  $\alpha_{\text{R}} = 0.75$  and  $\alpha_{\text{X}} = 1.2$ , they are the median synchrotron break frequency,  $\nu_{\text{br}} = 10^{14}$  Hz, the median equipartition magnetic field,  $B_{\text{eq}}(1) = 300 \mu\text{G}$ , and the median luminosity ratio,  $\eta \approx 0.02$ . Assuming hereafter a universal value of  $\eta = 0.01$  for all FR I sources, we are able to express the synchrotron luminosity of each knot (and hence to normalize the energy distribution of the synchrotron-emitting electrons for each knot) in terms of the total radio luminosity of the source. We further choose ‘typical’ values for the kinematic parameters of the jets at the position of the analyzed knots, namely a bulk Lorentz factor of  $\Gamma_{\text{j}} = 3$  and a jet viewing angle of  $\theta = 45^\circ$ . This particular (although sufficient for our purposes) choice is in agreement with the one-sidedness of the X-ray jets detected in FR I radio galaxies, and with the jet-counterjet radio brightness asymmetry for all the sources analyzed in this paper. Also, it results in a Doppler factor of the emitting plasma of  $\delta = 1$ , leading to  $B_{\text{eq}} = B_{\text{eq}}(1)$ .

With the above parameters, we reconstruct the energy distribution of the synchrotron-emitting electrons, and then compute their unabsorbed  $\gamma$ -ray emission due to IC scattering on the starlight photon field. We use formulae from Aharonian & Atoyan (1981), including the Klein-Nishina effects and relativistic velocity of the emitting plasma (see a detailed description in Stawarz et al. 2005). We assume a characteristic frequency of the starlight emission of  $\nu_{\text{star}} = 10^{14}$  Hz, and a bolometric starlight energy density at  $\sim 1$  kpc from the galactic center of  $U_{\text{star}} = 10^{-9}$  erg cm $^{-3}$ , both as measured in the host-galaxy rest frame (see Stawarz et al. 2003). The starlight radiation energy density then dominates the other photon fields in the jet rest frame, in particular the energy density of the synchrotron photons, by more than an order of magnitude for knot synchrotron luminosities  $\leq 10^{42}$  erg s $^{-1}$  and other parameters as discussed in the paper.

The resulting intrinsic IC luminosity,  $L_{\gamma}(\varepsilon)$ , consists of a power-law continuum  $\propto \varepsilon^{-0.75}$

at photon energies  $\varepsilon < 1 \text{ GeV}$ , a break region between  $1 \text{ GeV}$  and  $100 \text{ GeV}$  due to both the transition between the Thomson and the Klein-Nishina regimes and a break in the electron energy distribution, and finally a steep power-law for  $\varepsilon \geq 100 \text{ GeV}$  (see figure 1). With a maximum electron energy of  $E_e/m_e c^2 = 10^8$  assumed hereafter, the maximum IC photon energy is  $\varepsilon \approx 50 \text{ TeV}$ . Note that the energy density of the jet magnetic field in the emitting plasma rest frame (denoted by primes),  $U'_B = B_{\text{eq}}^2/8\pi \approx 3.6 \times 10^{-9} \text{ erg cm}^{-3}$ , is roughly comparable with the energy density of the starlight radiation,  $U'_{\text{star}} = \Gamma_j^2 U_{\text{star}} \approx 9 \times 10^{-9} \text{ erg cm}^{-3}$ , and hence the intrinsic IC luminosity is roughly comparable with the synchrotron luminosity. In particular, by integrating over the IC photon energy range,  $L_\gamma = \int_{\varepsilon_{\text{min}}}^{\varepsilon_{\text{max}}} L_\gamma(\varepsilon) d\varepsilon$ , we find that

$$L_\gamma \approx \left( \frac{\eta}{0.01} \right) \times L_{\text{tot}} \quad (2)$$

for  $\varepsilon_{\text{min}} = 100 \text{ MeV}$  and  $\varepsilon_{\text{max}} = 300 \text{ GeV}$ . Due to the specific spectral shape of the intrinsic IC emission, with a maximum at  $1 - 100 \text{ GeV}$ , the above relation is expected to be correct also for  $\varepsilon_{\text{min}} < 100 \text{ MeV}$  and  $\varepsilon_{\text{max}} > 300 \text{ GeV}$ . Obviously, the observed IC emission will be modified by the effects of absorption and subsequent re-processing of high-energy  $\gamma$ -ray photons on the diffuse cosmic background radiation fields, as described below.

## 2.2. Absorption and Re-processing of $\gamma$ -ray Photons

High-energy  $\gamma$ -ray photons produced at cosmological distances are likely to be absorbed by the diffuse cosmic background radiation due to photo-photon annihilation (Nikishov 1962; Gould & Schreder 1966; Stecker et al. 1992). The absorbed  $\gamma$ -rays are then re-emitted at lower energies due to inverse-Compton radiation of the created electron-positron pairs in the cascading process (Aharonian & Atoyan 1985; Protheroe 1986; Zdziarski 1988; Protheroe & Stanev 1993; Aharonian et al. 1994; Kel’Ner et al. 2004). Among other implications, this process is of significant interest in studying the contribution of cosmologically distant sources to the  $\gamma$ -ray background (Coppi & Aharonian 1997; Kneiske et al. 2005). A crucial point in the analysis of the attenuation of high-energy  $\gamma$ -rays emitted by cosmologically distant objects is, however, the knowledge of spectral shape of the MRF in the infrared-to-ultraviolet photon energy range, which is responsible for the  $\gamma$ -ray absorption/re-emission, and of its evolution up to high redshifts (see Primack et al. 1999). This is a complicated problem, since the direct measurements of the MRF at infrared wavelengths are difficult (see Hauser & Dwek 2001, and references therein). We note that careful analysis of the spectra of TeV-emitting blazars constitutes a very promising (although not direct, and, in addition, restricted to redshifts  $z < 1$ ) method for constraining unknown parameters of the MRF (e.g.,

Stanev & Franceschini 1998; Renault et al. 2001; Aharonian et al. 2002; Costamante et al. 2004; Dwek & Krennrich 2005).

Here we adopt a model proposed by Kneiske et al. (2002, 2004), which under a minimum of parameters and assumptions follows the evolution of the MRF from redshift  $z = 5$  to  $z = 0$ , fulfilling all the observational constraints on the MRF in the infrared-to-optical band at the present epoch. This forward evolution model based on optical and infrared galaxy surveys considers emission from stars, gas and dust in optically selected galaxies as well as in luminous and ultraluminous infrared galaxies (LIGs/ULIGs). The contribution of LIGs is essential, since the number of stars formed in this object is comparable to the one in optically selected galaxies, and their contribution to the infrared-to-ultraviolet metagalactic radiation field is about 50%. We note that in a framework of the adopted model the UV background is underestimated at redshifts  $z > 3$  by a factor of 2-4. With this for the MRF, we derive the optical depth for  $\gamma$ -ray absorption (including the effects of re-emission) as a function of redshift and  $\gamma$ -ray photon energy,  $\tau_{\gamma\gamma}(\varepsilon, z)$  (see Kneiske et al. 2005), and compute the observed absorbed IC flux of the selected FR I jets,

$$S_{\gamma}(\varepsilon) = \frac{(1+z)L_{\gamma}[(1+z)\varepsilon]}{4\pi d_L^2} \times \exp[-\tau_{\gamma\gamma}(\varepsilon, z)] \quad . \quad (3)$$

Figure 1 shows a comparison between the unabsorbed and the absorbed IC fluxes from kpc-scale jets located at different redshifts,  $z = 0.03, 0.1, 1.0,$  and  $4.0$  (for  $L_{\gamma} = 10^{41}$  ergs $^{-1}$ ). As illustrated, only a relatively small part of the IC flux is absorbed by the MRF in the 0.1 – 10 GeV photon energy range, and hence our analysis of the contribution of kpc-scale FR I jets to the  $\gamma$ -ray background radiation is not greatly affected by the inevitably somewhat arbitrary nature of the adopted MRF model.

### 2.3. $\gamma$ -ray Luminosity Function

We take the radio luminosity function — i.e. the number of sources per unit comoving volume per unit (base 10) logarithm of the source luminosity — characterizing low-power radio sources (including ‘classical’ FR I radio galaxies and FR II radio galaxies with weak/absent emission lines) in the form:

$$\rho_{\text{W}}(L, z) \equiv \frac{dN}{dV d \log L} = \begin{cases} \rho_0 \left(\frac{L}{L_{\text{cr}}}\right)^{-\alpha} \exp\left(\frac{-L}{L_{\text{cr}}}\right) (1+z)^k & \text{for } z < z_{\text{cr}} \\ \rho_0 \left(\frac{L}{L_{\text{cr}}}\right)^{-\alpha} \exp\left(\frac{-L}{L_{\text{cr}}}\right) (1+z_{\text{cr}})^k & \text{for } z \geq z_{\text{cr}} \end{cases} \quad (4)$$

as discussed by Willott et al. (2001). We adopt the values of the five free parameters of  $\rho_{\text{W}}(L, z)$  as determined from 3CRR, 6CE and 7CRS samples for a  $\Omega_{\text{M}} = \Omega_{\Lambda} = 0$  and

$H_0 = 50 \text{ km s}^{-1} \text{ Mpc}^{-1}$  cosmology by Willott et al. (2001, model C therein). We then convert this RLF to the modern cosmology adopted here, and convert the total radio luminosity to the IC jet luminosity  $L_\gamma$  according to equation 2. Hence, we obtain the  $\gamma$ -ray luminosity function for the jets in FR I radio galaxies, which can be written in the form

$$\rho(L_\gamma, z) = \kappa(z) \times \rho_W(L_\gamma, z) \quad , \quad (5)$$

where  $\log \rho_0 = -7.523$  (where  $\rho_0$  is in  $\text{Mpc}^{-3}$ ),  $\alpha = 0.586$ ,  $\log L_{\text{cr}} = 43.062$  (where  $L_{\text{cr}}$  is now the critical intrinsic  $\gamma$ -ray luminosity of the jet in  $\text{erg s}^{-1}$ ),  $z_{\text{cr}} = 0.71$ , and  $k = 3.48$ . The function  $\kappa(z)$  expresses the transformation of the comoving volume elements between different cosmological models,

$$\kappa(z) \equiv \frac{dV_W/d\Omega dz}{dV/d\Omega dz} \quad . \quad (6)$$

We note that

$$\frac{dV_W}{d\Omega dz} = \frac{c^3 z^2 (2+z)^2}{4 H_0^3 (1+z)^3} \quad \text{with} \quad H_0 = 50 \text{ km s}^{-1} \text{ Mpc}^{-1} \quad , \quad (7)$$

and

$$\frac{dV}{d\Omega dz} = \left(\frac{c}{H_0}\right)^3 E^{-1}(z) \left[\int_0^z \frac{dz'}{E(z')}\right]^2 \quad \text{with} \quad E(z) = \sqrt{\Omega_M (1+z)^3 + \Omega_\Lambda}, \quad (8)$$

$$H_0 = 71 \text{ km s}^{-1} \text{ Mpc}^{-1}, \quad \Omega_M = 0.27, \quad \text{and} \quad \Omega_\Lambda = 0.73 \quad .$$

The final form of  $\rho(L_\gamma, z)$  — shown in figure 2 (top panel) for redshifts  $z = 0.001, 1$  and  $2$  — gives then the number of low-power radio sources per unit comoving volume (in  $\text{Mpc}^3$ ) per unit (base 10) logarithm of the intrinsic IC jet luminosity  $L_\gamma$  (in  $\text{erg s}^{-1}$ ). We note that a similar approach to the luminosity function was adopted by Celotti & Fabian (2004), who discussed the *extended* X-ray emission of FR I radio galaxies (due to IC scattering of the cosmic microwave background radiation by radio-emitting electrons) in the context of deep X-ray surveys.

Figure 2 (bottom panel) shows also the cumulative number density of the low-power radio sources considered here,

$$\left(\frac{dN}{dV}\right)_{<z} \equiv \int_0^z dz' \int_{L_\gamma^{\text{low}}}^{L_\gamma^{\text{high}}} \frac{\rho(L_\gamma, z')}{L_\gamma \ln 10} dL_\gamma \quad , \quad (9)$$

as a function of redshift, for the set of  $L_\gamma^{\text{low}} = 10^{38} \text{ erg s}^{-1}$ ,  $10^{39} \text{ erg s}^{-1}$ ,  $10^{40} \text{ erg s}^{-1}$ , and  $L_\gamma^{\text{high}} = 10^{44} \text{ erg s}^{-1}$ . As illustrated, a change in the lowest luminosity of the GLF by an order of magnitude can change the number density of objects by a factor of about 3. Below we take  $L_\gamma^{\text{low}} = 10^{38} \text{ erg s}^{-1}$ , corresponding to the lowest 5 GHz luminosity of the whole

source  $L_{\text{tot}} = 10^{38} \text{ erg s}^{-1}$ , and note that the lack of such low-luminosity objects in our small observed ‘sample’ (Table 1) is most probably due to selection effects only. However, because of the very low  $\gamma$ -ray emission of such extremely low-power radio galaxies, the particular choice of  $L_{\gamma}^{\text{low}}$  will not substantially affect the following estimates. On the other hand, the number of high-luminosity sources in the population considered here, i.e., sources with a total radio power exceeding Fanaroff-Riley critical luminosity (roughly  $L_{\text{tot}} = 10^{42} \text{ erg s}^{-1}$ ), is negligible when compared to the number of lower-luminosity (‘classical’ FR I) objects. In other words, the adopted upper cut-off in the GLF,  $L_{\gamma}^{\text{high}} = 10^{44} \text{ erg s}^{-1}$ , can also be safely assumed in the following calculations. We finally note in this context, that X-ray jets with properties similar to the ‘classical’ FR I X-ray jets are indeed discovered in radio galaxies of intermediate power and morphology (e.g., 3C 15; Kataoka et al. 2003).

### 3. Results and Discussion

The  $\gamma$ -ray emission due to inverse-Compton scattering of starlight photons in the kpc-scale jets of FR I radio galaxies is relatively weak, accounting for only a small fraction of the direct EGRET measurement in the 0.1 – 10 GeV photon energy range, consistent with the analysis presented by Cillis et al. (2004). We note that for an EGRET sensitivity of  $5.4 \times 10^{-8} \text{ ph cm}^{-2} \text{ s}^{-1}$ , corresponding to a  $5\sigma$  detection in a one-year all-sky-survey (Bloom 1996), the ‘typical’ FR I kpc-scale jet as considered here could be eventually detected only if its luminosity distance is roughly  $d_L < 100 (L_{\gamma}/10^{44} \text{ erg s}^{-1})^{1/2} \text{ Mpc}$ . It does not mean, however, that the FR I jets cannot be associated with some unidentified EGRET sources, as the inverse-Comptonization of this and other photon fields (especially within the inner portions of the outflows) in some particular FR I objects can result in  $\gamma$ -ray signals exceeding the EGRET sensitivity (see in this context Mukherjee et al. 2002; Combi et al. 2003).

Promisingly, GLAST is expected to be a much more powerful instrument than EGRET, with the planned sensitivity for a  $5\sigma$  detection of a point source within the photon energy range 0.1 – 300 GeV in one-year all-sky-survey of  $1.5 \times 10^{-9} \text{ ph cm}^{-2} \text{ s}^{-1}$  (Bloom 1996). Thus, one should expect GLAST to observe at least a few FR I radio galaxies at redshifts  $z < 0.1$  due to the  $\gamma$ -ray emission of their brightest kpc-scale knots, if the jet parameters we assume are correct. In particular, the  $dN/dz$  distribution of the analyzed objects,

$$\left(\frac{dN}{dz}\right)_{\text{GL}} = 4\pi \int_{L_{\gamma}^{\text{GL}}}^{L_{\gamma}^{\text{high}}} \frac{dV}{d\Omega dz} \frac{\rho(L_{\gamma}, z)}{L_{\gamma} \ln 10} dL_{\gamma} \quad (10)$$

(where  $L_{\gamma}^{\text{GL}}$  corresponds to the minimum IC jet luminosity which would allow for a GLAST detection as discussed above), gives three observable FR I jets for  $L_{\gamma}^{\text{high}} = 10^{44} \text{ erg s}^{-1}$ .

Therefore, a GLAST survey covering low-power radio sources will be able to verify our simple model.

Meanwhile, the contribution of FR I jets to the EGRET  $\gamma$ -ray background can be evaluated for unresolved sources as

$$[\varepsilon I_\gamma(\varepsilon)] = \frac{4\pi}{\Omega_{\text{EG}}} \int_{z_{\text{min}}}^{z_{\text{max}}} \frac{dV}{d\Omega dz} dz \int_{L_\gamma^{\text{low}}}^{L_\gamma^{\text{high}}} \frac{\rho(L_\gamma, z)}{L_\gamma \ln 10} [\varepsilon S_\gamma(\varepsilon)] dL_\gamma \quad (11)$$

(e.g., Chiang et al. 1995), where  $\Omega_{\text{EG}} = 10.4$  is the solid angle covered by the survey,  $[\varepsilon S_\gamma(\varepsilon)]$  is the observed absorbed IC flux in  $\text{erg cm}^{-2} \text{s}^{-1}$  (equation 3), the comoving volume element  $dV/d\Omega dz$  is given by the equation 8, and the luminosity function  $\rho(L_\gamma, z)$  is given in the equation 5. The results are presented in figure 3: the jets in FR I radio galaxies (their brightest kpc-scale knots in particular) can contribute about one percent to the observed extragalactic  $\gamma$ -ray background in the 0.1–10 GeV photon energy range. Indeed, a much larger contribution by these objects is not expected, since accordingly to the analysis presented in, e.g., Kneiske et al. (2005), blazar sources can account for the bulk of the extragalactic  $\gamma$ -ray background. It indicates that the magnetic fields in the analyzed jet regions is not likely to be much smaller *on average* than the equipartition value, as otherwise the contribution of the considered objects would be uncomfortably high. Note that the IC jet luminosity scales roughly as  $L_\gamma \propto B^{-2}$ , and hence a magnetic field as low as 10  $\mu\text{G}$  would cause overproduction of the diffuse  $\gamma$ -ray background by the FR I jets on their own. Therefore, weak magnetic fields in the brightest kpc-scale knots in FR I jets can be excluded (see in this context Stawarz et al. 2005, for the case of M 87 jet).

There are a few significant features of our analysis. First, the analysis presented here does not depend on any particular model of particle acceleration in the jet, as the energy distribution of the radiating electrons is inferred directly from their synchrotron emission (see Stawarz et al. 2003, 2005). Second, we do not include here the inevitable synchrotron self-Compton process, which would increase the expected IC flux of the jets, especially in the ‘problematic’ (because of the absorption/re-processing effects) very high energy  $\gamma$ -ray band. Note also that, accordingly to our minimum-assumption approach, we consider the same equipartition value for the kpc-scale jet magnetic field in *all* FR I jets, which differ in total radio power (and hence most probably in jet kinetic luminosity) by several orders of magnitude. Indeed, for low-power jets one should expect an equipartition magnetic field of less than the 300  $\mu\text{G}$  obtained here for relatively powerful jets from our sample. In other words, we underestimate the inverse-Compton radiation of such extremely weak but numerous sources. Thus, the evaluated  $\gamma$ -ray emission can be considered as a *lower* limit only, and so the estimated one percent contribution to the extragalactic  $\gamma$ -ray background can be considered as *guaranteed*, as long as the minimum-power hypothesis for the kpc-scale

jets in FR I radio galaxies is correct.

Let us also mention that the presence of bright knots at  $\approx 1$  kpc from the active centers of FR I radio galaxies is indeed universal (Parma et al. 1987; Laing et al. 1999). These knots are usually called ‘flaring points’, since their positions always mark the transition in jet collimation and emissivity. Laing & Bridle (2002), who discussed the dynamics of the kpc-scale jet in the FR I radio galaxy 3C 31 in detail, concluded that the flaring points are most likely caused by the stationary reconfinement shocks formed due to rapid changes in pressure of the hot ambient gas (see also in this context, e.g., Sanders 1983; Falle & Wilson 1985; Komissarov 1994). Others attribute them to the Kelvin-Helmholtz instabilities, whose non-linear development can also result in the formation of weak oblique shocks (e.g., Hardee 1979; Bicknell & Begelman 1996; Lobanov et al. 2003). Whatever the case is, the analysis presented here suggests that a weak magnetic field at the position of the flaring points is unlikely. Of course, this conclusion is based on a simplified approach in modeling the IC emission of the kpc-scale FR I jets *on average*, and the jet parameters used in our analysis are determined from a relatively small sample of the X-ray emitting objects. However, more sophisticated analyses can be performed only with larger sample of FR I jets detected at optical and X-ray frequencies.

With the approximate lower limit of  $10 \mu\text{G}$ , the dynamical importance of the magnetic field in kpc-scale FR I jets cannot yet be determined, with additional uncertainty arising from the poorly known total kinetic powers of these outflows. In addition, any possible changes of the magnetic energy flux along the outflows are not constrained in our analysis. Let us only note in this context that modeling of the spectral energy distribution of BL Lac objects — believed to be beamed counterparts of FR I radio galaxies (Urry & Padovani 1995) — usually leads to sub-equipartition magnetic field characterizing the nuclear portion of the low-power jets (e.g., Kino et al. 2002), although the model uncertainties and variety in BL Lacs’ spectral properties are large. Hence, one can in principle suspect that amplification of the magnetic energy flux along the low-power jets between the sub-pc and kpc scales is required by the data, in agreement with the more detailed analysis of M 87 (Stawarz et al. 2005). We note that amplification of a mean magnetic energy flux is indeed expected in any conductive plasma containing non-vanishing helicity of turbulent motions or a strong velocity shear, although the general applicability of the simple kinematic dynamo theory — usually considered in this context — to realistic astrophysical situations (like the relativistic outflows discussed here) is not clear (see, e.g., the recent review by Vishniac et al. 2003).

L.S. was supported by the grants 1-P03D-011-26 and PBZ-KBN-054/P03/2001. T.M.K. was supported by the grant from the Australian Research Council. Authors acknowledge also very useful comments from P. Edwards, F. Aharonian, D. E. Harris, M. Ostrowski, and

A. Siemiginowska.

## REFERENCES

- Aharonian, F., & Atoyan, A. M. 1981, *Ap&SS*, 79, 321
- Aharonian, F. A., & Atoyan, A. M. 1985, *Soviet Phys.—JETP*, 62, 189
- Aharonian F. A., Coppi P. S., & Völk, H. J. 1994, *ApJ*, 423, L5
- Aharonian F. A., et al. 2002, *A&A*, 384, L23
- Bicknell, G. V., & Begelman, M. C. 1996, *ApJ*, 467, 597
- Bloom, E. D. 1996, *Space Sci. Rev.*, 75, 109
- Celotti, A., & Fabian, A. C. 2004, *MNRAS*, 353, 523
- Chiang, J., & Mukherjee, R. 1998, *ApJ*, 496, 752
- Chiang, J., Fichtel, C. E., von Montigny, C., Nolan, P. L., & Petrosian, V. 1995, *ApJ*, 452, 156
- Cillis, A. N., Hartman, R. C., & Bertsch, D. L. 2004, *ApJ*, 601, 142
- Combi, J. A., Romero, G. E., Paredes, J. M., Torres, D. F., & Ribo, M. 2003, *ApJ*, 588, 731
- Coppi, P. S., & Aharonian, F. A. 1997, *ApJ*, 487, 9
- Costamante, L., Aharonian, F., Horns, D., & Ghisellini, G. 2004, *NewAR*, 48, 469
- Dermer, C. D., & Schlickeiser, R. 1992, *Science*, 257, 1642
- Dwek, E., & Krennrich, F. 2005, *ApJ*, 618, 657
- Erlykin, A. D., & Wolfendale, A. W. 1995, *J. Phys. G*, 21, 1149
- Falle, S. A. E. G., & Wilson, M. J. 1985, *MNRAS*, 216, 79
- Gabici, S., & Blasi, P. 2003, *APh*, 19, 679
- Gould, R. J., & Schreder, G. 1966, *Phys. Rev. Lett.*, 16, 252
- Hardcastle, M. J., Birkinshaw, M., & Worrall, D. M. 2001, *MNRAS*, 326, 1499

- Hardcastle, M. J., Worrall, D. M., Birkinshaw, M., Laing, R. A., & Bridle, A. H. 2002, MNRAS, 334, 182
- Hardcastle, M. J., Worrall, D. M., Kraft, R. P., Forman, W. R., Jones, C., & Murray, S. S. 2003, ApJ, 593, 169
- Hardcastle, M. J., Worrall, D. M., Birkinshaw, M., Laing, R. A., & Bridle, A. H. 2005, MNRAS, 358, 843
- Hardee, P. E. 1979, ApJ, 234, 47
- Harris, D. E., Krawczynski, H., & Taylor, G. B. 2002a, ApJ, 578, 740
- Harris, D. E., Finoguenov, A., Bridle, A. H., Hardcastle, M. J., & Laing, R. A. 2002b, ApJ, 580, 110
- Hartman, R. C., et al. 1999, ApJS, 123, 79
- Hauser, M. G., & Dwek, E. 2001, ARA&A, 39, 249
- Jester S. 2003, NewAR, 47, 427
- Kataoka, J., & Stawarz, L. 2005, ApJ, 622, 797
- Kataoka, J., Leahy, J. P., Edwards, P. G., Kino, M., Takahara, F., Serino, Y., Kawai, N., & Martel, A. R. 2003, A&A, 410, 833
- Kel’Ner, S. R., Khangulyan, D. V., & Aharonian, F. A. 2004, Ast. L., 30, 663
- Kino, M., Takahara, F., Kusunose, M. 2002, ApJ, 564, 97
- Kneiske, T. M., Mannheim, K., & Hartmann, D. H. 2002, A&A, 386, 1
- Kneiske, T. M., Bretz, T., Mannheim, K., & Hartmann, D. H. 2004, A&A, 413, 807
- Kneiske, T., et al. 2005, in preparation
- Komissarov, S. S. 1994, MNRAS, 269, 394
- Kraft, R. P., Forman, W. R., Jones, C., Murray, S. S., Hardcastle, M. J., & Worrall, D. M. 2002, ApJ, 569, 54
- Laing, R. A., Parma, P., de Ruiter, H. R., & Fanti, R. 1999, MNRAS, 306, 513
- Laing, R. A., & Bridle, A. H. 2002, MNRAS, 336, 1161

- Liu, F. K., & Zhang, Y. H. 2002, *A&A*, 381, 757
- Lobanov, A., Hardee, P. E., & Eilek, J. 2003, *NewAR*, 47, 629
- Loeb, A., & Waxman, E. 2000, *Nature*, 405, 156
- Marshall, H. L., Miller, B. P., Davis, D. S., Perlman, E. S., Wise, M., Canizares, C. R., Harris, D. E., & Biretta, J. A. 2002, *ApJ*, 564, 683
- Mucke, A., & Pohl, M. 2000, *MNRAS*, 312, 177
- Mukherjee, R., Halpern, J., Mirabal, N., & Gotthelf, E. V. 2002, *ApJ*, 574, 693
- Nikishov, A. I. 1962, *Soviet Phys.—JETP*, 14, 393
- Padovani, P., Ghisellini, G., Fabian, A. C., & Celotti, A. 1993, *MNRAS*, 260, 21
- Parma, P., de Ruiter, H. R., Fanti, C., Fanti, R., & Morganti, R. 1987, *A&A*, 181, 244
- Primack, J.R., Bullock, J.S., Somerville, R.S., MacMinn, D. 1999, *APh*, 11, 93
- Protheroe, R. J. 1986, *MNRAS*, 221, 769
- Protheroe, R. J., & Stanev, T. 1993, *MNRAS*, 264, 191
- Renault, C., Barrau, A., Lagache, G., & Puget, J.-L. 2001, *A&A*, 371, 771
- Salamon, M. H., & Stecker, F. W. 1994, *ApJ*, 430, 21
- Sanders, R. H. 1983, *ApJ*, 266, 73
- Scarpa R., & Urry C. M. 2002, *NewAR*, 46, 405
- Setti, G. & Woltjer, L. 1994, *ApJS*, 92, 629
- Sparks W. B., Golombek D., Baum S. A., Biretta J., de Koff S., Macchetto F., McCarthy P., & Miley G. K. 1995, *ApJ*, 450, L55
- Sreekumar, P., et al. 1998, *ApJ*, 494, 523
- Stanev, T., & Franceschini, A. 1998, *ApJ*, 494, 159
- Stawarz, L., Sikora, M., & Ostrowski, M. 2003, *ApJ*, 597, 186
- Stawarz, L., Siemiginowska, A., Ostrowski, M. & Sikora, M. 2005, *ApJ*, 626, 120
- Stecker, F. W. & Salamon, M. H. 1996, *ApJ*, 464, 600

- Stecker, F. W., de Jager, O. C., & Salamon, M. H. 1992, *ApJ*, 390, L49
- Stecker, F. W., Salamon, M. H., & Malkan, M. A. 1993, *ApJ*, 410, 71
- Strong, A. W., Moskalenko, I. V., & Reimer, O. 2004, *ApJ*, 613, 956
- Urry, C. M., & Padovani, P. 1995, *PASP*, 107, 803
- von Montigny, C., et al. 1995, *ApJ*, 440, 525
- Vishniac, E. T., Lazarian, A., & Cho, J. 2003, in ‘Lecture Notes in Physics’ vol. 614, eds. E. Falgarone and T. Passot, p. 376, Springer-Verlag Berlin Heidelberg
- Weferling, B. & Schlickeiser, R. 1999, *A&A*, 344, 744
- Willott, C. J., Rawlings, S., Blundell, K. M., Lacy, M., & Eales, S. A. 2001, *MNRAS*, 322, 536
- Wilson, A. S., & Yang, Y. 2002, *ApJ*, 568, 133
- Worrall, D. M., Birkinshaw, M., & Hardcastle, M. J. 2001, *MNRAS*, 326, L7
- Worrall, D. M., Birkinshaw, M., & Hardcastle, M. J. 2003, *MNRAS*, 343, 73
- Zdziarski, A. A. 1988, *ApJ*, 335, 786

Table 1. Parameters for the brightest knots of the X-ray detected FR I jets.

name	$z$	$d_L$ [Mpc]	$\alpha_R$	$S_R$ [mJy]	$\alpha_X$	$S_X$ [nJy]	$S_O$ [ $\mu$ Jy]	$\log \nu_{br}$ [Hz]	$B_{eq}(1)$ [ $\mu$ G]	$\log L_{tot}$ [erg s $^{-1}$ ]	$\eta$
3C 15	0.073	326	0.85	55	1.2	1.2	1.6	14.16	877	42.0	0.035
NGC 315	0.0165	71	0.90	68	1.2	4.1	—	16.37	392	40.6	0.047
3C 31	0.0169	72	0.55	37	1.2	7.3	2.0	13.57	334	40.8	0.02
B 0206	0.0369	160	0.50	26	1.2	5.2	—	13.30	474	41.1	0.033
3C 66B	0.0215	92	0.60	34	1.2	6.2	15.8	13.84	374	41.3	0.01
3C 129	0.0208	89	0.75	3.8	1.2	1.9	—	16.19	196	41.1	0.001
B2 0755	0.0428	187	0.75	54	1.2	9.7	—	15.20	637	41.1	0.091
M 84	0.00354	15	0.65	13	1.2	1.16	<30	13.65	101	39.9	0.002
M 87	0.00427	18	0.70	2600	1.6	142	1000	15.29	510	41.3	0.024
Cen A	0.00081	3.4	0.75	520	1.5	110	—	16.17	125	40.8	0.0005
3C 296	0.0237	102	0.60	23.9	1.4	1.2	<10	14.02	358	41.0	0.015

Note. —  $z$ : redshift of the source,  $d_L$ : luminosity distance to the source adopting  $H_0 = 71 \text{ km s}^{-1} \text{ Mpc}^{-1}$ ,  $\Omega_m = 0.27$  and  $\Omega_\Lambda = 0.73$ .  $\alpha_R$ : radio spectral index at 5 GHz,  $S_R$ : radio flux density at 5 GHz in mJy,  $\alpha_X$ : X-ray spectral index at 1 keV,  $S_X$ : X-ray flux density at 1 keV in nJy,  $S_O$ : optical flux density at  $5 \times 10^{14}$  Hz in  $\mu$ Jy,  $\nu_{br}$ : break frequency of the synchrotron emission in Hz,  $B_{eq}(1)$ : the equipartition magnetic field computed for no relativistic beaming in  $\mu$ G,  $L_{tot}$ : total luminosity of the source at 5 GHz in erg s $^{-1}$ , and  $\eta$ : ratio between 5 GHz luminosity of the knot and total 5 GHz luminosity of the source. **References** — 3C 15: Kataoka et al. (2003); NGC 315: Worrall et al. (2003); 3C 31: Hardcastle et al. (2002); B 0206: Worrall et al. (2001); 3C 66B: Hardcastle et al. (2001); 3C 129: Harris et al. (2002a); B2 0755: Worrall et al. (2001); M 84: Harris et al. (2002b); M 87: Marshall et al. (2002); Wilson & Yang (2002); Cen A: Kraft et al. (2002); Hardcastle et al. (2003); 3C 296: Hardcastle et al. (2005). Total radio luminosities are taken from Liu & Zhang (2002) and converted to the adopted cosmology and an observing frequency of 5 GHz.

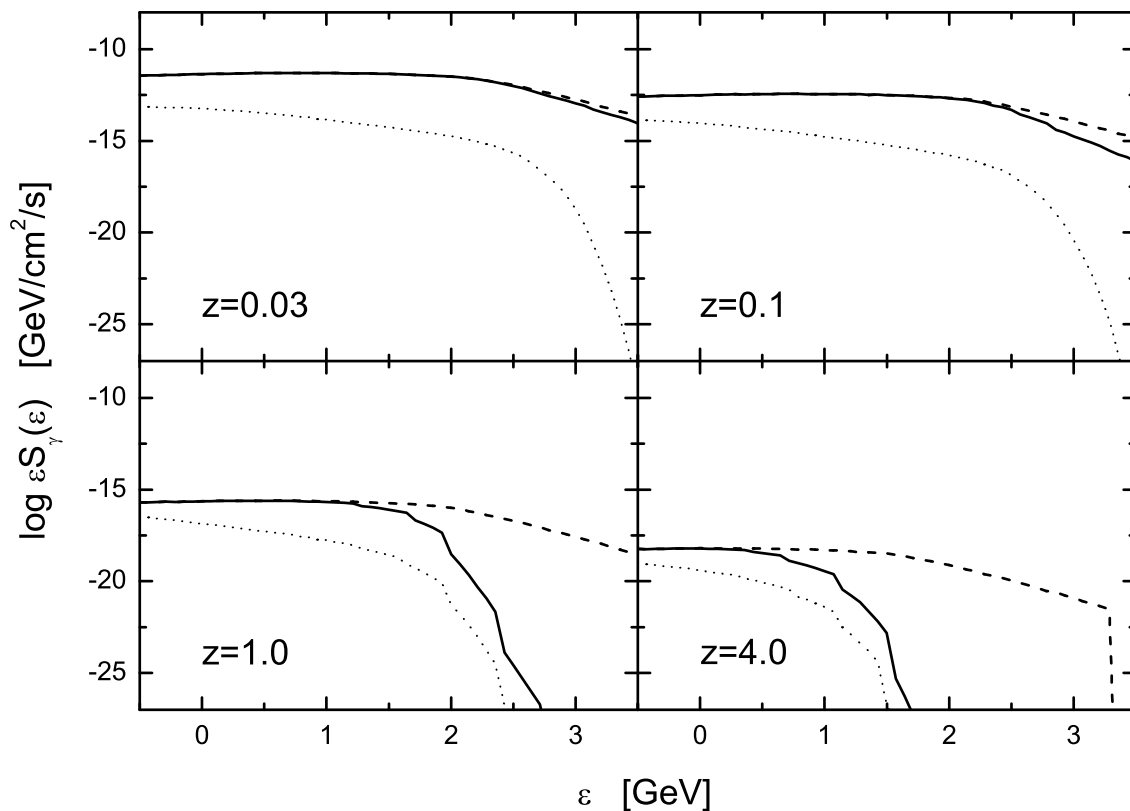


Fig. 1.—  $\gamma$ -ray spectra of kpc-scale FR I jets located at redshifts  $z = 0.03, 0.1, 1.0$  and  $4.0$  (as indicated at each panel) for a total IC jet luminosity  $L_\gamma = 10^{41} \text{ erg s}^{-1}$ . Dashed lines indicate emission intrinsic to the source, thick solid lines correspond to the emission which would be measured by the observer located at  $z = 0$  (with absorption/re-emission effects included), while dotted lines illustrate emission from the source’s halo.

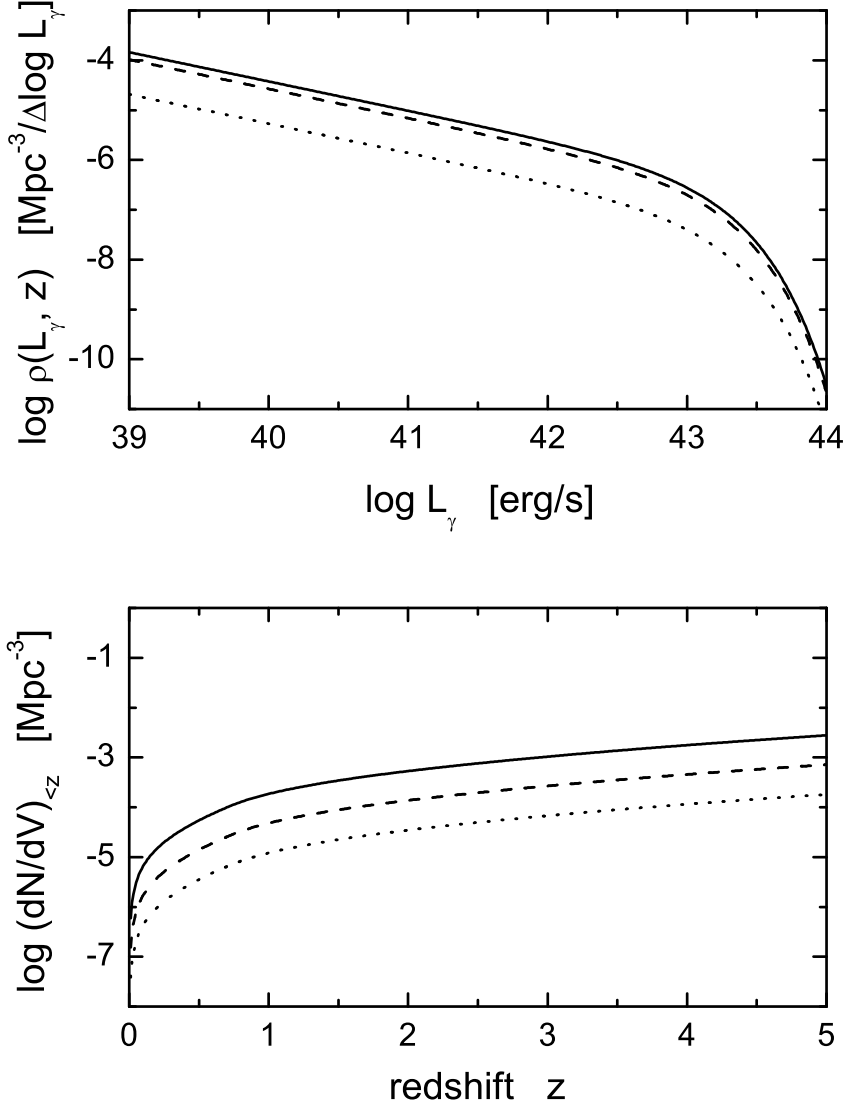


Fig. 2.— *top*: GLF of kpc-scale FR I jets for a modern cosmology ( $\Omega_M = 0.27$ ,  $\Omega_\Lambda = 0.73$ ,  $H_0 = 71 \text{ km s}^{-1} \text{ Mpc}^{-1}$ ) and redshifts  $z = 0.001$ , 1, and 2 (dotted, dashed and solid lines, respectively) as a function of total IC jet luminosity  $L_\gamma$ . *bottom*: Cumulative number density of low-power radio sources as a function of redshift, for  $L_\gamma^{\text{low}} = 10^{38} \text{ erg s}^{-1}$ ,  $10^{39} \text{ erg s}^{-1}$  and  $10^{40} \text{ erg s}^{-1}$  (solid, dashed and dotted lines, respectively), and  $L_\gamma^{\text{high}} = 10^{44} \text{ erg s}^{-1}$ .

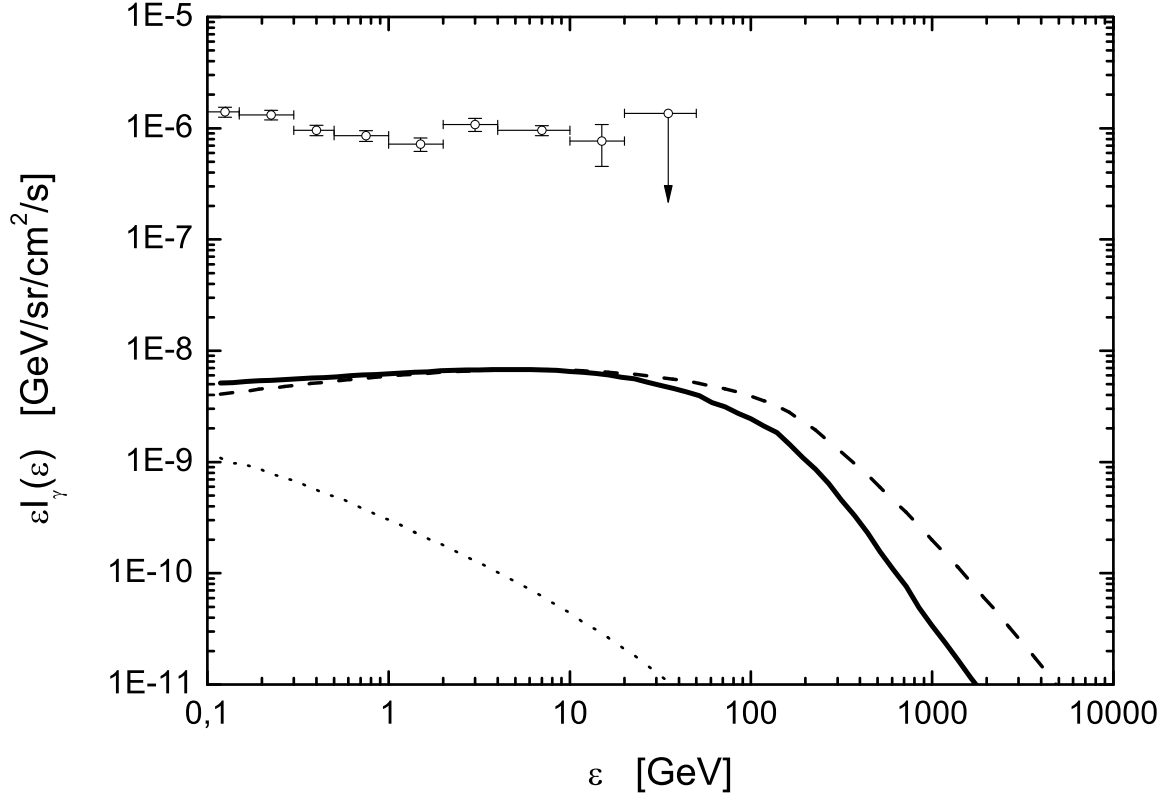


Fig. 3.— Contribution of FR I kpc-scale jets to the extragalactic  $\gamma$ -ray background for  $z_{\min} = 0$ ,  $z_{\max} = 5$ ,  $L_{\gamma}^{\text{low}} = 10^{38} \text{ erg s}^{-1}$ , and  $L_{\gamma}^{\text{high}} = 10^{44} \text{ erg s}^{-1}$  (lines denoted as in figure 1). Open circles correspond to the extragalactic EGRET  $\gamma$ -ray background as determined by Strong et al. (2004).